HHS Public Access

Author manuscript

J Mot Behav. Author manuscript; available in PMC 2017 December 17.

Published in final edited form as:

J Mot Behav. 2017 ; 49(3): 312–328. doi:10.1080/00222895.2016.1204265.

Grasp-Based Functional Coupling Between Reach- and Grasp-Related Components of Forelimb Muscle Activity

Shashwati Geed[1,2,3] and **Peter L. E. van Kan**[1]

[1]Department of Kinesiology, University of Wisconsin–Madison, Wisconsin

[2]MedStar National Rehabilitation Hospital, Washington, DC

[3]Department of Rehabilitation Medicine, Georgetown University Medical Center, Washington, DC

Abstract

How are appropriate combinations of forelimb muscles selected during reach-to-grasp movements in the presence of neuromotor redundancy and important task-related constraints? The authors tested whether grasp type or target location preferentially influence the selection and synergistic coupling between forelimb muscles during reach-to-grasp movements. Factor analysis applied to 14–20 forelimb electromyograms recorded from monkeys performing reach-to-grasp tasks revealed 4–6 muscle components that showed transport/preshape- or grasp-related features. Weighting coefficients of transport/preshape-related components demonstrated strongest similarities for reaches that shared the same grasp type rather than the same target location. Scaling coefficients of transport/preshape- and grasp-related components showed invariant temporal coupling. Thus, grasp type influenced strongly both transport/preshape- and grasp-related muscle components, giving rise to grasp-based functional coupling between forelimb muscles.

Keywords

grasping; motor control; multijoint control; temporal coupling

Reach-to-grasp movements require precise spatiotemporal coordination between proximal forelimb muscles that transport the hand to the target, and distal muscles that preshape the hand and grasp. Control of multijoint behaviors such as reaching to grasp is complex because of the large number of degrees of freedom to be controlled (Bernstein, 1967), and because task-related parameters constrain the selection of muscles and differentially affect their patterns of activation. For example, target shape, size, and orientation during grasp influence activity of hand muscles (Brochier, Spinks, Umilta, & Lemon, 2004; Overduin, d'Avella, Roh, & Bizzi, 2008; Winges, Kundu, Soechting, & Flanders, 2007), whereas the location of the target in the limb's workspace influences activity of shoulder and elbow muscles (d'Avella, Fernandez, Portone, & Lacquaniti, 2008; d'Avella & Lacquaniti, 2013;

Correspondence address: Shashwati Geed, MedStar National Rehabilitation Hospital, 102 Irving St. NW, Washington, DC 20010. sg1075@georgetown.edu.

Color versions of one or more of the figures in the article can be found online at www.tandfonline.com/vjmb.

d'Avella, Portone, Fernandez, & Lacquaniti, 2006; Flanders, 1991; Flanders, Pellegrini, & Geisler, 1996; Flanders, Pellegrini, & Soechting, 1994; Saltiel, Wyler-Duda, D'Avella, Tresch, & Bizzi, 2001). How the neuromotor system selects appropriate combinations of forelimb muscle activities in the presence of neuromotor redundancy and the necessity to accommodate task-related requirements differentially on subsets of muscles is a central and as yet unresolved question in motor control.

An increasing body of evidence supports the view that modular components underlying muscle activity, called synergies, defined as functionally-related groups of muscles activated in fixed proportions with respect to each other and controlled as a unit, underlie the complexity and diversity of motor behaviors (Cheung et al., 2012; d'Avella & Lacquaniti, 2013; d'Avella et al., 2006; Klein Breteler, Simura, & Flanders, 2007; Mason, Gomez, & Ebner, 2001; Overduin, d'Avella, Carmena, & Bizzi, 2012; 2014; Overduin et al., 2008; Santello, Baud-Bovy, & Jöorntell, 2013; Tresch & Jarc, 2009; Weiss & Flanders, 2004; Yakovenko, Krouchev, & Drew, 2011). Synergies, however, do not necessarily address the computational complexity of control arising from redundancy (Diedrichsen & Classen, 2012). Synergies may themselves be activated in a potentially large number of combinations, unless the neuromotor circuitry implements rules governing the preferential selection, activation, or coupling between synergies. Identifying which task-related parameters yield relatively stronger influences on the selection and activation of synergies can give better mechanistic insights into how behavioral features influence control of forelimb musculature.

In the present study, we identified components of reach-to-grasp muscle activity using the computational framework of muscle synergies in order to examine the degree to which task-related parameters preferentially influence selection and synergistic coupling between transport/preshape- and grasp-related muscle activity. Specifically, we evaluated the relative importance of two task-related parameters, (a) type of grasp (precision or whole hand) and (b) target location, in preferential activation of transport/preshape-related components and their coupling with grasp-related components. Since grasp type and target location impose different behavioral demands on proximal and distal forelimb muscles, does one or the other parameter preferentially influence how combinations of proximal and distal muscles are coupled synergistically for reach-to-grasp movements? A finding that transport/preshape-related components of muscle activity are more similar when reaches share the same grasp type than when they share the same target location would imply that grasp type is more important than target location for selection of transport/preshape-related components of forelimb muscle activity. Our results support this hypothesis, underscoring the overall importance of intended hand use in the control of reach-to-grasp behaviors.

The present study differs from previous studies focused on muscle synergies underlying reach-to-grasp movements (d'Avella et al., 2008; d'Avella & Lacquaniti, 2013; d'Avella et al., 2006; d'Avella, Portone, & Lacquaniti, 2011; Overduin et al., 2008; Russo, D'Andola, Portone, Lacquaniti, & d'Avella, 2014; Sabatini, 2002). Whereas previous studies focused on demonstrating that a limited number of muscle synergies or components underlie the diversity of reach-to-grasp behaviors, in the present study we determined the extent to which two task-related parameters important for control of reaching to grasp preferentially influence the selection of muscle components underlying reach-to-grasp behaviors in an

effort to understand the control principles governing spatiotemporal coordination of reach-to-grasp movements.

Methods

We studied electromyographic (EMG) activity of fore-limb muscles of two purpose-bred male rhesus monkeys *(Macaca mulatta,* 7-10 kg) during various reach-to-grasp tasks. All animal care and experimental procedures complied with the U.S. Public Health Service Policy on Humane Care and Use of Laboratory Animals, conformed to the National Institutes of Health Guide for the Care and Use of Laboratory Animals, and were approved by the Institutional Animal Care and Use Committee of the University of Wisconsin-Madison.

Experimental Protocol

Two monkeys (B, W) were trained to perform stereotyped reach-to-grasp tasks that varied in two parameters that are important to reach-to-grasp coordination: (a) spatial location of the target, to the left of, above, to the right of, or below the shoulder of the trained limb (left, up, right, or down, respectively; Figure 1A), and (b) type of grasp (precision, or whole hand) required to complete the task (Figures 1B and 1C). Starting from a common location at the waist, the monkeys reached to grasp a food reward (Kellogg's Froot Loops cereal, Kellogg's, Battle Creek, MI; thickness: ~6 mm, diameter: ~19 mm) in one of four locations within the workspace of the trained limb. The monkeys retrieved the cereal from either a horizontally oriented narrow slot (height: 6 mm, width: 25 mm, depth: 25 mm), which required apposition of the thumb and index finger in a precision grip, or from a 50-ml glass beaker (height: 40 mm, diameter: 32 mm). The beaker was tilted at a 45° angle toward the animal and retrieval of the cereal required concerted use of the four fingers in a whole-hand grasp.

Reach-to-grasp movements started from a common location at the waist, where the monkeys held a handle while receiving small amounts of water reward. Illumination of one of the two light-emitting diodes (LEDs; one mounted next to the horizontal slot, the other mounted next to the beaker) at each of the four target locations instructed the type of grasp required, and cued the animal to initiate the reach-to-grasp movement. Simultaneous with illumination of the LED, the cereal was dispensed in either the slot or beaker, and the animal released the handle, reached for and grasped the cereal, placed the cereal in its mouth, and returned its hand to the starting location at its waist. The next trial was initiated following a variable (3–5 s) intertrial interval.

Reach-to-grasp movements were instructed in a pseudorandom sequence. There were no repeat movements to the same target location in subsequent trials. Reach-to-grasp trials alternated between whole hand and precision.

Behavioral and EMG Recordings

Behavioral Event Markers

Behavioral event times were recorded with contact sensors on the handle at the starting location at the waist, and on the slot and beaker at the target location. Reach onset and offset were defined as the times of breaking contact with the handle and making contact with the slot or beaker, respectively. Behavioral event times were used to normalize the durations of transport/preshape and grasp phases across trials and to align trials.

EMG Activity

We recorded EMG activity from 14 (monkey W) and 20 (monkey B) shoulder, elbow, wrist, and digit muscles with percutaneously implanted bipolar EMG electrodes (Table 1).

EMG activity was collected in sets of nine muscles per session on different days in close succession. EMG signals were rectified, integrated (time constant: 10 ms), band-pass filtered (30 Hz to 3 kHz), and digitized at 167 Hz by A/D computer inputs (CED 1401 plus, Cambridge Electronic Design, Cambridge, England). Data processing and analyses were carried out using custom software (MatLab 6.5, The MathWorks, Natick, MA).

EMG Signal Processing

We recorded eight sets of EMG data for each of the two animals: four target locations (left, up, right, and down) and two grasp types (precision and whole hand). Rectified and filtered EMG signals were low-pass filtered using a fourth-order Butterworth filter with a cutoff frequency of 15 Hz. Standardized records of EMG activity of a given muscle for a given target location and grasp type remained consistent over multiple trials and recording sessions, which ensured that the particular combinations of nine muscles/recording session in which EMGs were recorded did not influence the outcome in terms of the muscles that were a part of the same muscle component. Consistent activation patterns of EMGs also allowed us to combine EMG data across trials and recording sessions as described subsequently.

Each individual reach-to-grasp trial was divided into four phases: premovement, transport/preshape, grasp, and return. The premovement phase consisted of a 250-ms interval prior to reach onset. The transport/preshape phase was defined as the interval between reach onset and reach offset. The grasp phase was defined as the interval between reach offset (grasp onset) and grasp offset. The return phase consisted of a 250-ms interval immediately following grasp offset during which the animal placed the cereal in its mouth and grasped the handle at its waist in order to initiate the next trial.

Trials with outlier durations of either the transport/preshape or grasp phase were removed using Rosner's Many Outliers Procedure (Rosner, 1983). The number of trials removed ranged from 1 of 87 (1.2%) to 6 of 84 (7.1%) in monkey W, and from 0 of 40 (0%) to 6 of 44 (13.6%) in monkey B. We computed the mean duration of transport/preshape and grasp phase across the remaining trials for an animal, and time-normalized the transport/preshape and grasp phases to their respective mean durations. Individual trials for a given target

location and grasp type were aligned to reach onset and averaged across trials. Time-normalized, trial-averaged EMGs were then standardized to have zero mean and unit standard deviation in order to center and normalize the distributions of EMG activity across muscles as required for factor analysis.

Data Analysis

Extracting Components of Muscle Activity

Exploratory factor analysis (EFA) with varimax factor rotation was applied to the correlation matrix of standardized EMG records for each target location and grasp type (Tabachnick & Fidell, 2013). The goal of applying EFA is to represent EMG data (D × t matrix, where D is the number of muscles in the dataset, and m(t) is the EMG activity of a given muscle at each point in time (t) as linear combination of N factors, or muscle components, with N < D such that

$$m(t) = \sum_{i=1}^{N} c_i(t)\, w_i$$

where w_i (D × N matrix) represents the weighting coefficients representing the relative strength of activation of muscles in the i-th component. Weighting coefficients w_i range between C1 and –1, with values close to C1 reflecting strongly increased, and values close to –1 reflecting reduced muscle activation within a component. $c_i(t)$ represents the time-varying (temporal) scaling coefficient of a given component of muscle activity, reflecting the time course of activation of the i-th muscle component throughout the reach-to-grasp task.

The number of muscle components to retain following factor analysis was decided based on the (a) Kaiser criteria (Kaiser, 1974) and (b) scree plot of extracted components (Cattell, 1966). The combined criteria ensured that factors retained in the final solution contributed to meaningful interpretation of muscle activity in the context of reaching to grasp, and accounted for a sizable amount of variance in the EMG data, whereas factors with relatively small contributions (i.e., factors representing noise) were excluded.

We applied the factor analysis to the correlation matrix of standardized EMG records to ensure that every muscle in the analysis was weighted equally irrespective of extraneous factors such as the relative scale of muscle activation amplitude, frequency or order in which the EMGs were recorded, and size of the muscle. In summary, the following two factors ensured that the particular set of muscles sampled in a given recording session did not influence the composition of muscle components extracted by factor analysis: (a) consistent patterns of the standardized records of EMG activity of a given muscle across recording sessions and (b) use of correlation matrix of standardized EMG data in the factor analysis.

Temporal Coupling Between Transport/Preshape- and Grasp-Related Components—We classified the components of muscle activity as either transport/preshape- or grasp-related based on the combination of two criteria: (a) time of maximal contribution of the component scaling coefficients and (b) combination of muscles

contributing strongly to the component weighting coefficients ($w_i > 0.4$), as detailed in the Results section. Visual examination of scaling coefficients of transport/preshape- and grasp-related components suggested temporal coupling such that time of peak activation of the transport/preshape-related component was coincident with time of peak slope of activation of its corresponding grasp-related component (see Table 3). We therefore identified the times of peak activation of transport/preshape-related components, and peak slope of activation of grasp-related components, and tested their synchronicity using a paired-samples *t* test. Specifically, we tested the null hypothesis that there is no significant difference between the time of peak activation of transport/preshape-related component, and peak slope of activation of its corresponding grasp-related component of muscle activity.

To exclude the possibility that a coincident temporal relationship between components of transport/preshape-and grasp-related muscle activities resulted from the orthogonal relationship between factors extracted using varimax factor rotation during EFA, we also extracted muscle components using promax factor rotation, which does not constrain the components to be orthogonal. Promax factor rotation resulted in similar temporal scaling coefficients and coupling between transport/preshape- and grasp-related components of reach-to-grasp muscle activity, suggesting that the functional coupling between transport/preshape-and grasp-related components did not depend their orthogonal relationship.

Strength of Association Between Transport/Preshape-Related Components— We quantified the strength of association between pairs of transport/preshape-related components of muscle activity across tasks by computing the R_v coefficient (Escoufier, 1973; Robert & Escoufier, 1976).

$$R_v(X,Y) = \frac{tr\left(XX'YY'\right)}{\sqrt{\left(tr(XX')^2 tr(YY')^2\right)}}$$

where X and Y are matrices of weighting coefficients w_i of transport/preshape-related components of muscle activities. The R_V coefficients range between 0 and 1 with values closer to 1 indicating stronger association between matrices, and hence stronger similarity between components of muscle activities. The permutation test developed by Josse, Pages, and Husson (2008) was used to assess the statistical significance of the R_V coefficient by testing the null hypothesis that there is no significant association between matrices X and Y. R_V coefficients were computed, and their statistical significance was evaluated with the CoeffRv routine in R's FactoMineR package (Lê, Josse, & Husson, 2008).

To aid interpretation of the observed distribution of R_V coefficients, pairs of transport/preshape-related components of reach-to-grasp muscle activity were analyzed in greater detail by applying a complete-linkage hierarchical cluster analysis to the cosine distance d (X, Y) between components. Cosine distances between components were derived from the R_V coefficients as follows (Abdi, 2007):

$$d(X,Y)=\frac{XX'}{\left(tr\left(XX'^{2}\right)^{\frac{1}{2}}\right)}-\frac{YY'}{\left(tr\left(YY'^{2}\right)^{\frac{1}{2}}\right)}=\sqrt{2}\sqrt{1-R_v(X,Y)}$$

Cosine distances were used to create a step-wise hierarchical cluster tree in which muscle components most similar to each other (i.e., components with the smallest cosine distance) were merged into a single cluster. The distance matrix was then updated and the next step of clustering was performed until all muscle components merged into a single cluster. The updated distances between newly formed clusters were computed using the furthest-neighbors method (Everitt, 2010) in which distances between clusters are defined as the greatest distance between any two objects in the different clusters. We present results from the furthest-neighbors method of clustering; however, single- and weighted-average update rules for merging clusters showed the same cluster patterns, suggesting that the identified clusters were robust and did not depend on the specific clustering algorithm used.

Results

The two monkeys performed reach-to-grasp movements to retrieve cereal rewards. Movements varied systematically in target location (left, up, right, or down) and type of grasp (precision or whole hand). Target locations and grasp types were presented in a pseudorandom sequence such that there were no repeat movements to the same target location in subsequent trials, and grasp type alternated between whole hand and precision.

For each task condition, we used exploratory factor analysis to extract between four and six muscle components that explained > 85% of the variance in EMG records of 14-20 forelimb muscles (Table 2). Muscle components showed transport/preshape- or grasp-related features, characterized based on muscles contributing heavily to the factor weighting coefficients w_i and activation times of the components' temporal scaling coefficients $c_i(t)$.

The following sections report four main results of this study. First, the muscle components we identified showed functional specificity, contributing predominantly to the transport/preshape or grasp phase of reach-to-grasp movements. Second, the temporal scaling coefficients $c_i(t)$ of muscle components remained invariant across tasks and individual animals. Third, the scaling coefficients $c_i(t)$ of transport/preshape- and grasp-related components of muscle activity were temporally coupled with each other such that time of peak activation of a given transport/preshape-related component was coincident with the time of peak slope of activation of its corresponding grasp-related component for both animals during the reach-to-grasp tasks. Fourth, both transport/preshape- and grasp-related components of muscle activity showed specificity for intended type of hand use (a) the weighting coefficients w_i of transport/preshape-related components were preferentially coupled with a given type of grasp rather than a given target location and (b) the weighting coefficients w_i of grasp-related components were specific for the type of grasp irrespective of grasp location in the workspace.

Functional Specificity of Muscle Components

Transport/preshape-related components of muscle activity were characterized by temporal scaling coefficients that attained maxima during the transport/preshape phase of reaching to grasp, and relatively strong contributions from either proximal or combination of proximal and distal fore-limb muscles (weighting coefficients $w_i > 0.4$). Grasp-related components of muscle activity were characterized by temporal scaling coefficients that attained maxima during the latter half of transport/preshape or grasp phase of reaching to grasp and relatively strong contributions from distal forelimb muscles either in isolation or in combination with proximal muscles. Figure 2 shows component scaling coefficients as a function of time for the first four muscle components during each task and in each monkey.

Component 1 (Figure 2A) and component 2 (Figure 2B) show transport/preshape-related activity in both monkeys. The two components increase in activation amplitude at or prior to reach onset, attain peak amplitude during the transport/preshape phase prior to or at the time the hand makes contact with the target, and sharply decrease the amplitude of activation during the latter half of the transport/preshape phase or early in the grasp phase. Activation of component 1 remains at relatively low levels throughout the grasp and return phase. In contrast, activation amplitude of component 2 steadily increases during the grasp phase and attains a second peak late in the grasp phase or during early return when the hand is moved closer to the mouth in order to ingest the food reward.

Component 3 (Figure 2C) and component 4 (Figure 2D) show grasp-related activity in both monkeys. Component 3 attained peak amplitude early in the grasp phase near the time the hand contacted the target and remained active at a relatively high amplitude throughout the first two-thirds (precision) or first half (whole hand) of the grasp phase. Component 4 in monkey W was identified in both precision and whole hand tasks and was associated with episodes of increased wrist and digit flexion during the reach-to-grasp movement. A sharp relatively brief phasic increase in activity of component 4 occurred during the premovement phase immediately prior to reach onset, which corresponded with the monkey grasping the handle at the start location. A second peak in activation amplitude, at the onset of the grasp phase was more prominent during the whole hand than precision task, and a third rapid increase in activity occurred at the onset of the return phase when the animal started to move the hand towards the mouth to ingest the food reward. The corresponding grasp-related component 4 in monkey B was identified in the whole hand task to the right and down targets; however, it did not meet our a priori criteria for selection as a muscle component in the other task conditions.

We characterized components 1 and 2 as mainly transport/preshape related and components 3 and 4 as mainly grasp related based on the major influences in their component weighting and temporal scaling coefficients. For accurately characterizing a muscle component's contribution, it is critical to cross reference (a) the component's maximal contribution during transport/preshape and grasp phase with (b) the combination of muscles contributing strongly to the component weighting coefficients ($w_i > 0.4$, the conventionally accepted cutoff for strong contribution to a factor in factor analysis and structural equation modeling (O'Rourke, Psych, & Hatcher, 2013). However, we must note that each of the muscle components contributes throughout the reach-to-grasp movement with some degree of

overlap between transport/preshape and grasp. Thus, our characterization of a muscle component as transport/preshape- or grasp-related does not preclude its smaller contributions to the other phase of movement.

Invariance of Component Activation Waveforms

We assessed the extent of similarity between component scaling coefficients across tasks and animals quantitatively by computing pairwise correlations for each of the eight task conditions. Linear correlation coefficients are summarized in the color matrices of Figure 3. We considered correlation magnitudes > 0.5 or < –0.5 to represent strong correlations, magnitude ranging from 0.3 to 0.5 or –0.3 to –0.5 to represent moderate correlations, and between –0.3 and 0.3 to represent relatively weak correlations (Portney & Watkins, 2009). Components 1 and 3 demonstrated strong pairwise correlations suggesting that the scaling coefficients of reach-to-grasp-related component 1 (transport/preshape-related) and component 3 (grasp-related) are well conserved across tasks and animals (Figures 3A and 3C). The few exceptions were for activation waveforms associated with a few specific task conditions (component 1: up and down targets in precision task for monkey W; component 3: right and down targets in whole hand task for monkey B). Invariance of scaling coefficients of muscle components 1 and 3 across tasks and animals is particularly remarkable because, as reported below, the weighting coefficients of muscle components 1 and 3 varied across tasks and animals.

Pairwise correlations of temporal scaling coefficients for component 2 in monkey W (Figure 3B) were moderate to strong for nearly all comparisons indicating invariance across tasks. Temporal scaling coefficients for component 2 in monkey B were highly correlated within a given task (i.e., for movements that shared the same grasp type) but were uniformly weak for comparison across tasks (Figure 3B). Results for comparison of component 2's similarity across monkeys were mixed suggesting relatively greater specificity of the component for a given animal in contrast with components 1 and 3 that showed generalized invariance across animals. Temporal scaling coefficients associated with component 4 (identified in monkey W but not in monkey B) were correlated strongly within a grasp type, and showed moderate to strong correlations across grasp types (Figure 3D). Thus, correlations were relatively stronger within a task (i.e., for movements that shared the same grasp type rather than target location) indicating that the scaling coefficient associated with component 4 was grasp-specific and did not depend on the location of grasp in the monkey's workspace.

Temporal Coupling Between Transport/Preshape-and Grasp-Related Components

Visual inspection of activation waveforms of scaling coefficients for component 1 (Figure 2A) and component 3 (Figure 2C) suggested temporal coupling: peak activation of component 1 occurred in close temporal synchrony with peak slope of activation of component 3 (Table 3). Figure 4 illustrates the temporal coupling between components 1 and 3 for precision and whole hand tasks in monkey W and monkey B. We formally tested the hypothesis of invariant temporal coupling between scaling coefficients of transport/preshape- and grasp-related components of reach-to-grasp muscle activities using a paired-samples *t* test. The *t* test showed no significant difference, $t(15) = 0.06$, $p = .96$) between the time of peak activation of component 1 ($M = 0.28$, $SD = 0.06$) and time of peak slope of

activation of component 3 ($M = 0.28$, $SD = 0.06$) during the transport/preshape phase of both animals in both tasks. Thus, scaling coefficients of components 1 and 3 (transport/preshape- and grasp-related, respectively) are temporally coupled with each other irrespective of tasks or animals. Since each muscle component is comprised of behaviorally relevant functional combinations of proximal and distal muscles that are activated in fixed ratios with respect to each other (as detailed below), the temporal coupling between transport/preshape- and grasp-related components of muscle activity will result in precise spatiotemporal coordination between the muscles included in the coupled components.

Influence of Grasp Type on Composition of Muscle Components

Factor analysis indicates that the weighting coefficients w_i of each of the components, whether transport/preshape-or grasp-related, define characteristic combinations of distal and proximal forelimb muscles.

Component 1 in monkey W (Figures 5A and 5B) was characterized by strong contributions from proximal muscles with coactivation of wrist and digit muscles (precision: FCU, FDS, ECR, EDC; whole hand: FCU and EDC) for some target locations. Component 2 in monkey W (Figures 5C and 5D) included shoulder and elbow muscles with weighting coefficients that were strongly dependent on target location (precision and whole hand: PEC, TRI, BIC; precision: SpDLT) in combination with wrist and digit muscles (precision: ECR, FDS, EDC; whole hand: FCU, APL, ECR, EDC).

Component 1 in monkey B (Figures 6A and 6B) included strong contributions from the proximal shoulder and elbow muscles that were common to precision and whole hand tasks along with coactivation of wrist (precision: FCR, ECR; whole hand: FCU, FCR, ECR) and digit muscles (precision: PL, APL, ED23; whole hand: PL, APL, ED45, ED23, EDC). Component 2 in monkey B derived from TM and BR in the precision task and from BR, AcDLT, and SpDLT in the whole-hand task (Figures 6C and 6D). These proximal muscles acted in concert with various combinations of wrist and digit muscles (precision: ECR, APL, EPL, PL, FDS, ED23, EDC; whole hand: ECU, ECR, EPL, FDP, ED45, ED23, EDC).

In summary, the combined results support a functional contribution of muscle components 1 and 2 to transporting the hand towards the target while stabilizing, opening, and shaping the hand in preparation for grasp.

Transport/Preshape-Related Components of Reach-to-Grasp Muscle Activity Are Preferentially Selected Based on Grasp Type

To test the hypothesis that transport/preshape-related components of muscle activity are preferentially selected based on grasp type rather than target location, we computed the strength of similarity between pairs of transport/preshape-related components of muscle activity across tasks using the R_V coefficient. Transport/preshape-related components showed significant pairwise similarities across tasks; but the R_V coefficients were higher, and therefore, strength of association between transport/preshape-related components of muscle activity across tasks was stronger when reaches shared the same grasp type than when reaches shared the same target location (Figures 7A and 7B).

To reveal the specific features underlying strength of similarity demonstrated by R_V coefficients, we applied hierarchical cluster analysis (furthest-neighbors method) to the cosine distance between weighting coefficients of the transport/preshape-related components of muscle activity. Cluster algorithms group objects that are most similar given a set of distances between the objects. One can tap into the latent features underlying similarity between objects by studying properties of objects that are clustered together. The hierarchical tree obtained from clustering divided into two main branches that grouped transport/preshape-related components into two main clusters, based on the patterns of grasp type (Figures 7C and 7D). Thus, in both animals, the transport/preshape-related components of reach-to-grasp-related muscle activity was more similar for reaches that shared the same grasp type than for reaches that shared the same target location.

Specificity of Grasp-Related Components of Muscle Activity

Spatial composition of grasp-related components (3 and 4) was distinct and specific for grasp type. The precision task required extension of the metacarpophalangeal (MCP) joints and flexion of the interphalangeal (IP) joints (Figure 1C). Consistent with this pattern of hand use, muscle component 3 in precision included EDC and FDP in monkey W (Figure 8A), and a predominance of wrist-digit extensors and flexors (FCU, FDP) in monkey B (Figure 8C) in combination with particular proximal muscles (AcDLT and SpDLT in monkey W, and BR in monkey B). In contrast, the whole-hand task involved overall flexion movement of the hand (Figure 1B). Accordingly, spatial composition of grasp-related component 3 was biased in favor of digit and palmar flexor muscles (monkey W: FDS, FDP, PL; monkey B: FDS, FDP, FCU, PL with ED45 and ECU) in combination with particular proximal muscles (monkey W: AcDLT, SpDLT, TRI; monkey B: AcDLT, SpDLT) (Figure 8B; Figure 8D).

Weighting coefficients of component 4 in monkey W (Figures 9A and 9B) included distal flexor muscles (FCR, FCU, PL, FDS, and APL) with minor contributions of BIC and PEC. Component 4 in monkey B (Figure 9C) included wrist and digit flexors (FCU, FDP) and extensors (ECU, EC45, ED23, EPL) in combination with AcDLT and BR. Thus, grasp-related components of muscle activity during reach-to-grasp movements are distinct and specific for the type of grasp, irrespective of the location of grasp in the fore-limb's workspace.

Discussion

We set out to determine the extent to which target location or type of intended hand use (grasp type) preferentially influence the selection and synergistic coupling between transport/preshape- and grasp-related components of fore-limb muscle activity. Given the neuromotor redundancy, and differential influence of task-related parameters on subsets of forelimb muscles, how does the neuromotor circuitry select appropriate combinations of muscle activities for coordinated reach-to-grasp movements?

We used the dimension-reduction properties of factor analysis to simplify the description of forelimb EMG activity and study whether one or the other task-related parameters preferentially influenced forelimb control during reaching to grasp. We extracted between

four and six components of reach-to-grasp-related EMG activity from 14 or 20 forelimb muscles recorded while two monkeys performed reach-to-grasp tasks that systematically varied in target location and grasp type. The extracted components of muscle activity explained at least 85% of the variability in EMG records in each monkey and demonstrated functional specificity, contributing predominantly to either the transport/preshape- or grasp-related aspects of reach-to-grasp movements.

Our use of dimension reduction in the context of fore-limb muscle activity differs from recent reports exploring muscle synergies in reach-to-grasp movements (d'Avella et al., 2008; d'Avella & Lacquaniti, 2013; d'Avella et al., 2006; d'Avella et al., 2011; Overduin et al., 2008; Russo et al., 2014; Sabatini, 2002; Tresch & Jarc, 2009) because our study focuses on the rules governing selection, activation, and synergistic coupling between combinations of proximal and distal forelimb muscles rather than the low-dimensional, modular control of reach-to-grasp movements. Identifying the rules governing preferential selection and activation of muscle patterns is critical to a mechanistic understanding of how behavioral demands interact with neuromotor circuitry for coordinated movements.

Importance of Intended Hand Use to Control of Forelimb Muscle Activity During Reaching to Grasp

The weighting coefficients of muscle components we identified highlight two important features of forelimb muscle activation during reaching to grasp: (a) the muscle components reflect functional combinations of proximal and distal muscles suggesting that forelimb muscles are controlled as integrated units during reaching to grasp, and (b) both transport/preshape- and grasp-related muscle components are strongly influenced by intended hand use (grasp type). Hand-biased control of the forelimb is advantageous for several reasons. The hand is the fore-limb's end effector; therefore, hand use essentially determines how we engage with our environment. Moreover, the hand encompasses the largest number of independent degrees of freedom in the forelimb (Soechting & Flanders, 1997), which makes it most efficient for the neuromotor control system to plan forelimb movements according to how hand-related degrees of freedom must be engaged to accomplish behavioral goals. Furthermore, most forelimb reaching movements involve precise manipulation of hand joints while proximal muscles transport, orient, or stabilize the hand, making it essential to control proximal forelimb muscles in the context of hand use.

Our results showing influence of grasp type on spatial and temporal properties of muscle components during reach-to-grasp movements in the two monkeys compare reasonably well with previous reports examining components of forelimb muscle activity (Brochier et al., 2004; Overduin et al., 2008). Both studies reported that up to three muscle synergies (or principal components) explained at least 81% of the variance in EMG activity of 12 or 19 forelimb muscles recorded while monkeys performed reach-to-grasp tasks, which is consistent with our finding that between four and six components explain up to 85% of the variance in 14–20 forelimb EMGs. Consistent with our finding that type of grasp influences muscle components underlying reach-to-grasp tasks, both studies observed the influence of object size or shape (which monkeys were carefully trained to grasp using distinct grasp types) on the components underlying forelimb muscle activities. Overduin et al. (2008)

reported that each of the three synergies they identified was significantly modulated in its scaling and/or timing coefficients by object size and/or shape. Brochier et al. (2004) found that EMG activity of forelimb muscle activity was specifically tuned for object shapes. A combination of the first five principal components Brochier et al. (2004) identified correctly predicted a majority of reach-to-grasp trials as belonging to a particular object at times as early as 40–50% of the movement duration. Early identification of intended grasp type from muscle activations during transport is not surprising considering our finding that the transport/preshape-related components of reach-to-grasp muscle activities show specificity for the types of grasp and therefore, transport/preshape-related components of muscle activity contain information related to the patterns of intended hand use.

Temporal Coupling Between Transport/Preshape-and Grasp-Related Components

Temporal scaling coefficients of the muscle components dictate how each muscle included in the component will be activated because the muscles included in a component are activated synchronously and in fixed ratios with respect to each other. The temporal scaling coefficients for components 1 and 3 remained invariant across tasks and animals, whereas components 2 and 4 showed relatively greater specificity for the type of grasp or particular animal. Invariant scaling coefficients for components 1 and 3 are especially noteworthy because we recorded different forelimb muscles in the two monkeys (Table 1), and the spatial weighting coefficients of components 1 and 3 are different across animals and tasks. Muscle components with invariant temporal scaling coefficients but different weighting coefficients suggests that these temporal scaling coefficients could act as generalized global templates to coordinate motor behaviors when the appropriate weighting coefficients are selected; analogously, invariance of temporal scaling coefficients of muscle components in the lower limb has been identified in locomotion as well (Ivanenko, Poppele, & Lacquaniti, 2004).

Further, our finding that temporal scaling coefficients for components 1 and 3 are coupled in time across tasks and animals implies invariant coupling between functional units of movement, in this case, between transport/preshape- and grasp-related components of muscle activity. Functional coupling between kinematic aspects of transport (wrist velocity) and grasp (grip aperture—the distance between thumb and index finger during reaching to grasp) are well established (Jeannerod, 1981, 1984); however, analogous EMG-based correlates of functional coupling between transport/preshape- and grasp-related aspects of reach-to-grasp movements have been difficult to define because of the complexity and diversity of forelimb EMG activity during reaching to grasp, until now. Our use of dimension-reduction properties of factor analysis on forelimb EMG activity led to a relatively simpler description of the EMG data while retaining the variability of forelimb EMG activity, which allowed us to identify invariant functional coupling between EMG-based correlates of transport/preshape and grasp.

To eliminate the possibility that the observed invariant temporal coupling between transport/preshape- and grasp-related components is a consequence of their orthogonal relationship resulting from the varimax factor rotation, we also extracted muscle components using a nonorthogonal rotation (promax, oblique rotation). We found no differences between

temporal scaling coefficients of components extracted using the promax versus the varimax rotation, thereby eliminating the possibility that the temporal coupling between transport/preshape- and grasp-related components of forelimb EMG activity is a consequence of their orthogonal nature.

Implications for Neural Control of Reach-to-Grasp Behaviors

Our finding that the coupling between proximal and distal muscles is based on patterns of intended hand use is consistent with the encoding characteristics of cells throughout the neural circuitry that contributes critically to the control of reach-to-grasp movements. Neurons in the nucleus interpositus (van Kan, Horn, & Gibson, 1994), the sole output from intermediate cerebellum, and its target, the magnocellular red nucleus (van Kan & McCurdy, 2001, 2002) show the strongest discharge modulations for whole-limb movements that require hand use. Primary motor cortical (Dum & Strick, 1996; McKiernan, Marcario, Karrer, & Cheney, 1998; Park, Belhaj-Saif, & Cheney, 2004; Park, Belhaj-Saif, Gordon, & Cheney, 2001; Rathelot & Strick, 2009) and rubrospinal neurons (Belhaj-Saif, Karrer, & Cheney, 1998) make strong, direct, and more frequent projections to spinal circuitry that innervates either hand, or combinations of arm and hand muscles, which is consistent with the proximal-distal coupling and distal bias we observed in the control of fore-limb muscle components underlying reach-to-grasp movements.

Clinically, patients with stroke show the most severe hemiparesis in wrist and digit muscles (Colebatch & Gandevia, 1989). However, during the acute stage, motor control of grasp is not any more disrupted than motor control of reach (Lang et al., 2005), contrary to what one would expect given the strength of distal hemiparesis poststroke (Colebatch & Gandevia, 1989) and proximal to distal gradient of descending corticospinal terminations (Dum & Strick, 1996, 2002; Lemon, 2008). The relatively similar degree of impairment in reach and grasp components of reach-to-grasp movements in spite of a strong proximal to distal gradient in the underlying neuromotor connectivity are explained by our findings that show hand-based synergistic coupling between proximal and distal muscles, although differences between human and nonhuman primate neurophysiology must be noted.

Further, neurons in premotor areas F2 and F5, critical for control of reach-to-grasp movements, encode grasp types (Raos, Umilta, Gallese, & Fogassi, 2004; Raos, Umilta, Murata, Fogassi, & Gallese, 2006), and F5 projections to the primary motor cortex (M1) modulate their neural output in a grasp-specific manner (Davare, Lemon, & Olivier, 2008; Prabhu et al., 2009). Our finding of grasp-specific muscle components is in direct agreement with the prospect that descending commands via M1 preserve the grasp specificity observed in F5-M1 projections and encode muscle components specific to intended hand use (Holdefer & Miller, 2002; Morrow & Miller, 2003; Overduin et al., 2012).

Conclusion

Forelimb muscle activity during reach-to-grasp movements can be explained using a few (4–6) muscle components that align with transport/preshape- or grasp-related aspects of reach-to-grasp movements. The temporal scaling coefficients of transport/preshape (component 1) and grasp (component 3) show global invariance across tasks and animals suggesting that

they serve as templates for spatiotemporal coordination between reach and grasp. This result is further supported by our finding that these global invariant components are temporally coupled with each other, and may serve as the EMG-based correlates of the well documented kinematic coupling between transport and grasp (Jeannerod, 1981, 1984; Paulignan, Frak, Toni, & Jeannerod, 1997; Paulignan, Jeannerod, MacKenzie, & Marteniuk, 1991; Paulignan, MacKenzie, Marteniuk, & Jeannerod, 1991). Further, when reaching to grasp, the neuromotor circuitry specifies muscle activity patterns throughout the forelimb in the context of intended patterns of hand use because transport/preshape- and grasp-related components of forelimb muscle activities demonstrated relatively stronger influences of the type of grasp as compared to the location of grasp in the workspace.

Acknowledgments

The authors thank Robert P. Scobey for design and construction of experimental equipment and Janet L. Ruhland for assistance in data collection. They also thank Barbara S. Bregman, Michelle L. Harris-Love, Peter S. Lum, Sahana N. Kukke, and Susan Ryerson for valuable discussions and feedback on the manuscript. This research was conducted in the Motor Systems Physiology Laboratory at the University of Wisconsin-Madison in partial fulfillment of Shashwati Geed's PhD degree.

Funding: The work was supported by National Institute of Neurological Disorders and Stroke Grant [NS43317], (Peter L. E. van Kan), the Graduate School of the University of Wisconsin-Madison (Peter L. E. van Kan), National Institute of Neurological Disorders and Stroke Grant [1U10NS086513-01], (NIH StrokeNet, PI: Alexander W. Dromerick, and Amie Hsia, MedStar National Rehabilitation Hospital, and Georgetown University), and National Institute on Disability, Independent Living, and Rehabilitation Research Advanced Rehabilitation Research Training Grant [H133P100015] (PI: Barbara Bregman, MedStar National Rehabilitation Hospital, and Georgetown University).

References

Abdi, H. RV and congruence coefficients. In: Salkind, NJ., Rasmussen, K., editors. Encyclopedia of measurement and statistics. Thousand Oaks, CA: Sage; 2007. p. 849-853.

Belhaj-Saif A, Karrer JH, Cheney PD. Distribution and characteristics of poststimulus effects in proximal and distal forelimb muscles from red nucleus in the monkey. Journal of Neurophysiology. 1998; 79:1777–1789. [PubMed: 9535947]

Bernstein, NA. The co-ordination and regulation of movements. New York, NY: Pergamon Press; 1967.

Brochier T, Spinks RL, Umilta MA, Lemon RN. Patterns of muscle activity underlying object-specific grasp by the macaque monkey. Journal of Neurophysiology. 2004; 92:1770–1782. [PubMed: 15163676]

Cattell RB. The scree test for the number of factors. Multivariate Behavioral Research. 1966; 1:245–276. http://dx.doi.org/10.1207/s15327906mbr0102_10. [PubMed: 26828106]

Cheung VC, Turolla A, Agostini M, Silvoni S, Bennis C, Kasi P, et al. Bizzi E. Muscle synergy patterns as physiological markers of motor cortical damage. Proceedings of the National Academy of Sciences of the USA. 2012; 109:14652–14656. http://dx.doi.org/10.1073/pnas.1212056109. [PubMed: 22908288]

Colebatch JG, Gandevia SC. The distribution of muscular weakness in upper motor neuron lesions affecting the arm. Brain. 1989; 112:749–763. [PubMed: 2731028]

d'Avella A, Fernandez L, Portone A, Lacquaniti F. Modulation of phasic and tonic muscle synergies with reaching direction and speed. Journal of Neurophysiology. 2008; 100:1433–1454. http://dx.doi.org/10.1152/jn.01377.2007. [PubMed: 18596190]

d'Avella A, Lacquaniti F. Control of reaching movements by muscle synergy combinations. Frontiers in Computational Neuroscience. 2013; 7:42. http://dx.doi.org/10.3389/fncom.2013.00042. [PubMed: 23626534]

d'Avella A, Portone A, Fernandez L, Lacquaniti F. Control of fast-reaching movements by muscle synergy combinations. The Journal of Neuroscience. 2006; 26:7791–7810. http://dx.doi.org/10.1523/JNEUROSCI.0830–06.2006. [PubMed: 16870725]

d'Avella A, Portone A, Lacquaniti F. Superposition and modulation of muscle synergies for reaching in response to a change in target location. Journal of Neurophysiology. 2011; 106:2796–2812. http://dx.doi.org/10.1152/jn.00675.2010. [PubMed: 21880939]

Davare M, Lemon R, Olivier E. Selective modulation of interactions between ventral premotor cortex and primary motor cortex during precision grasping in humans. The Journal of Physiology. 2008; 586:2735–2742. http://dx.doi.org/10.1113/jphysiol.2008.152603. [PubMed: 18403420]

Diedrichsen J, Classen J. Stimulating news about modular motor control. Neuron. 2012; 76:1043–1045. http://dx.doi.org/10.1016/j.neuron.2012.12.001. [PubMed: 23259939]

Dum RP, Strick PL. Spinal cord terminations of the medial wall motor areas in macaque monkeys. The Journal of Neuroscience. 1996; 16:6513–6525. [PubMed: 8815929]

Dum RP, Strick PL. Motor areas in the frontal lobe of the primate. Physiology & Behavior. 2002; 77:677–682. http://dx.doi.org/10.1016/S0031-9384(02)00929–0. [PubMed: 12527018]

Escoufier Y. Le traitement des variables vectorielles. Biometrics. 1973; 29:751–760. http://dx.doi.org/10.2307/2529140.

Everitt, B. Cluster analysis. Oxford: Wiley-Blackwell; 2010.

Flanders M. Temporal patterns of muscle activation for arm movements in three-dimensional space. The Journal of Neuroscience. 1991; 11:2680–2693. [PubMed: 1880544]

Flanders M, Pellegrini JJ, Geisler SD. Basic features of phasic activation for reaching in vertical planes. Experimental Brain Research. 1996; 110:67–79. [PubMed: 8817258]

Flanders M, Pellegrini JJ, Soechting JF. Spatial/temporal characteristics of a motor pattern for reaching. Journal of Neurophysiology. 1994; 71:811–813. [PubMed: 8176443]

Holdefer RN, Miller LE. Primary motor cortical neurons encode functional muscle synergies. Experimental Brain Research. 2002; 146:233–243. http://dx.doi.org/10.1007/s00221-002–1166-x. [PubMed: 12195525]

Ivanenko YP, Poppele RE, Lacquaniti F. Five basic muscle activation patterns account for muscle activity during human locomotion. The Journal of Physiology. 2004; 556:267–282. http://dx.doi.org/10.1113/jphysiol.2003.057174. [PubMed: 14724214]

Jeannerod, M. Intersegmental coordination during reaching at natural visual objects. In: Long, J., Baddeley, A., editors. Attention and performance. Vol. IX. Hillsdale, NJ: Erlbaum; 1981. p. 153-169.

Jeannerod M. The timing of natural prehension movements. Journal of Motor Behavior Impact Factor & Description. 1984; 16:235–254.

Josse J, Pages J, Husson F. Testing the significance of the RV coefficient. Computational Statistics & Data Analysis. 2008; 53:82–91. http://dx.doi.org/10.1016/j.csda.2008.06.012.

Kaiser H. An index of factorial simplicity. Psychometrika. 1974; 39:31–36. http://dx.doi.org/10.1007/BF02291575.

Klein Breteler MD, Simura KJ, Flanders M. Timing of muscle activation in a hand movement sequence. Cerebral Cortex. 2007; 17:803–815. http://dx.doi.org/10.1093/cer-cor/bhk033. [PubMed: 16699078]

Lang CE, Wagner JM, Bastian AJ, Hu Q, Edwards DF, Sahrmann SA, Dromerick AW. Deficits in grasp versus reach during acute hemiparesis. Experimental Brain Research. 2005; 166:126–136. http://dx.doi.org/10.1007/s00221-005-2350-6. [PubMed: 16021431]

Le S, Josse J, Husson F. FactoMineR: An R package for multivariate analysis. Journal of Statistical Software. 2008; 25 Retrieved from https://www.jstatsoft.org/index.php/jss/article/view/v025i01/v25i01.pdf.

Lemon RN. Descending pathways in motor control. Annual Review of Neuroscience. 2008; 31:195–218. http://dx.doi.org/10.1146/annurev.neuro.31.060407.125547.

Mason CR, Gomez JE, Ebner TJ. Hand synergies during reach-to-grasp. Journal of Neurophysiology. 2001; 86:2896–2910. [PubMed: 11731546]

McKiernan BJ, Marcario JK, Karrer JH, Cheney PD. Corticomotoneuronal postspike effects in shoulder, elbow, wrist, digit, and intrinsic hand muscles during a reach and prehension task. Journal of Neurophysiology. 1998; 80:1961–1980. [PubMed: 9772253]

Morrow MM, Miller LE. Prediction of muscle activity by populations of sequentially recorded primary motor cortex neurons. Journal of Neurophysiology. 2003; 89:2279–2288. http://dx.doi.org/10.1152/jn.00632.2002. [PubMed: 12612022]

O'Rourke, N., Psych, R., Hatcher, L. A step-by-step approach to using SAS for factor analysis and structural equation modeling. Cary, NC: SAS Institute; 2013.

Overduin SA, d'Avella A, Carmena JM, Bizzi E. Microstimulation activates a handful of muscle synergies. Neuron. 2012; 76:1071–1077. http://dx.doi.org/10.1016/j.neuron.2012.10.018. [PubMed: 23259944]

Overduin SA, d'Avella A, Carmena JM, Bizzi E. Muscle synergies evoked by microstimulation are preferentially encoded during behavior. Frontiers in Computational Neuroscience. 2014; 8:20. http://dx.doi.org/10.3389/fncom.2014.00020. [PubMed: 24634652]

Overduin SA, d'Avella A, Roh J, Bizzi E. Modulation of muscle synergy recruitment in primate grasping. The Journal of Neuroscience. 2008; 28:880–892. http://dx.doi.org/10.1523/JNEUROSCI.2869–07.2008. [PubMed: 18216196]

Park MC, Belhaj-Saif A, Cheney PD. Properties of primary motor cortex output to forelimb muscles in rhesus macaques. Journal of Neurophysiology. 2004; 92:2968–2984. http://dx.doi.org/10.1152/jn.00649.2003. [PubMed: 15163675]

Park MC, Belhaj-Saif A, Gordon M, Cheney PD. Consistent features in the forelimb representation of primary motor cortex in rhesus macaques. The Journal of Neuroscience. 2001; 21:2784–2792. [PubMed: 11306630]

Paulignan Y, Frak VG, Toni I, Jeannerod M. Influence of object position and size on human prehension movements. Experimental Brain Research. 1997; 114:226–234. [PubMed: 9166912]

Paulignan Y, Jeannerod M, MacKenzie C, Marteniuk R. Selective perturbation of visual input during prehension movements. 2. The effects of changing object size. Experimental Brain Research. 1991; 87:407–420. [PubMed: 1769391]

Paulignan Y, MacKenzie C, Marteniuk R, Jeannerod M. Selective perturbation of visual input during prehension movements. 1. The effects of changing object position. Experimental Brain Research. 1991; 83:502–512. [PubMed: 2026193]

Portney, LG., Watkins, MP. Foundations of clinical research: Applications to practice. Boston, MA: Pearson/Prentice Hall; 2009.

Prabhu G, Shimazu H, Cerri G, Brochier T, Spinks RL, Maier MA, Lemon RN. Modulation of primary motor cortex outputs from ventral premotor cortex during visually guided grasp in the macaque monkey. The Journal of Physiology. 2009; 587:1057–1069. http://dx.doi.org/10.1113/jphysiol.2008.165571. [PubMed: 19139043]

Raos V, Umilta MA, Gallese V, Fogassi L. Functional properties of grasping-related neurons in the dorsal premo-tor area F2 of the macaque monkey. Journal of Neurophysiology. 2004; 92:1990–2002. http://dx.doi.org/10.1152/jn.00154.2004. [PubMed: 15163668]

Raos V, Umilta MA, Murata A, Fogassi L, Gallese V. Functional properties of grasping-related neurons in the ventral pre-motor area F5 of the macaque monkey. Journal of Neurophysiology. 2006; 95:709–729. http://dx.doi.org/10.1152/jn.00463.2005. [PubMed: 16251265]

Rathelot JA, Strick PL. Subdivisions of primary motor cortex based on cortico-motoneuronal cells. Proceedings of the National Academy of Sciences of the USA. 2009; 106:918–923. http://dx.doi.org/10.1073/pnas.0808362106. [PubMed: 19139417]

Robert P, Escoufier Y. A unifying tool for linear mul-tivariate statistical methods: The RV-coefficient. Journal of the Royal Statistical Society. Series C (Applied Statistics). 1976; 25:257–265. http://dx.doi.org/10.2307/2347233.

Rosner B. Percentage points for a generalized ESD many-outlier procedure. Technometrics. 1983; 25:165–172. http://dx.doi.org/10.2307/1268549.

Russo M, D'Andola M, Portone A, Lacquaniti F, d'Avella A. Dimensionality of joint torques and muscle patterns for reaching. Frontiers in Computational Neuroscience. 2014; 8:24. http://dx.doi.org/10.3389/fncom.2014.00024. [PubMed: 24624078]

Sabatini AM. Identification of neuromuscular synergies in natural upper-arm movements. Biological Cybernetics. 2002; 86:253–262. http://dx.doi.org/10.1007/s00422-001–0297-7. [PubMed: 11956806]

Saltiel P, Wyler-Duda K, D'Avella A, Tresch MC, Bizzi E. Muscle synergies encoded within the spinal cord: evidence from focal intraspinal NMDA iontophoresis in the frog. Journal of Neurophysiology. 2001; 85:605–619. [PubMed: 11160497]

Santello M, Baud-Bovy G, J€orntell H. Neural bases of hand synergies. Frontiers in Computational Neuroscience. 2013; 7:23. http://dx.doi.org/10.3389/fncom.2013.00023. [PubMed: 23579545]

Soechting JF, Flanders M. Flexibility and repeatability of finger movements during typing: analysis of multiple degrees of freedom. Journal of Computational Neuroscience. 1997; 4:29–46. [PubMed: 9046450]

Tabachnick, BG., Fidell, LS. Using multivariate statistics. Boston, MA: Pearson Education; 2013.

Tresch MC, Jarc A. The case for and against muscle synergies. Present Opinion in Neurobiology. 2009; 19:601–607. http://dx.doi.org/10.1016/j.conb.2009.09.002.

van Kan PL, Horn KM, Gibson AR. The importance of hand use to discharge of interpositus neurones of the monkey. The Journal of Physiology. 1994; 480:171–190. [PubMed: 7853221]

van Kan PL, McCurdy ML. Role of primate magno-cellular red nucleus neurons in controlling hand preshaping during reaching to grasp. Journal of Neurophysiology. 2001; 85:1461–1478. [PubMed: 11287470]

Van Kan PL, McCurdy ML. Contribution of primate magnocellular red nucleus to timing of hand preshaping during reaching to grasp. Journal of Neurophysiology. 2002; 87:1473–1487. [PubMed: 11877520]

Weiss EJ, Flanders M. Muscular and postural synergies of the human hand. Journal of Neurophysiology. 2004; 92:523–535. http://dx.doi.org/10.1152/jn.01265.2003. [PubMed: 14973321]

Winges SA, Kundu B, Soechting JF, Flanders M. Intrinsic hand muscle activation for grasp and horizontal transport. Eurohaptics. 2007; 1:39–43. http://dx.doi.org/10.1901/jaba.2007.1–39. [PubMed: 20407618]

Yakovenko S, Krouchev N, Drew T. Sequential activation of motor cortical neurons contributes to intralimb coordination during reaching in the cat by modulating muscle synergies. Journal of Neurophysiology. 2011; 105:388–409. http://dx. doi.org/10.1152/jn.00469.2010. [PubMed: 21068260]

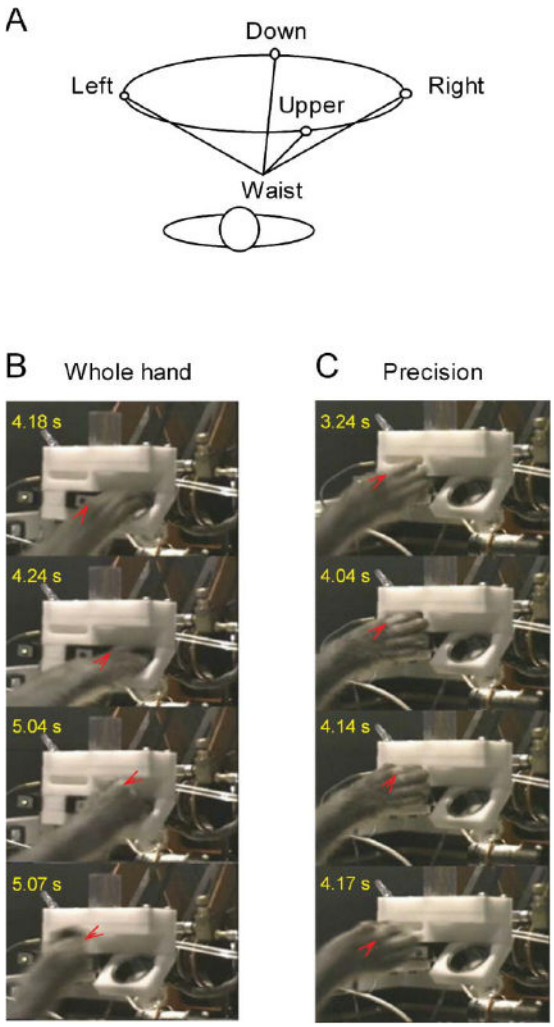

Figure 1.

Reach-to-grasp task. A. Geometrically accurate 3-D top view of the target locations relative to the animal's waist and shoulders. Two target locations (left, and right) were at shoulder height at angles of 31° to the left and 28° to the right of the parasagittal plane through the shoulder. The other two target locations (up and down) were within the sagittal plane through the shoulder at angles of 56° above and 5° below the horizontal plane through the shoulder. B-C: Video frames showing the animal's hand during task performance. Red arrowheads point to the metacarpophalangeal (MCP) joint of the index finger. The whole-hand task required flexion of the interphalangeal (IP) and MCP joints to retrieve the cereal from the beaker. The precision task required flexion of the IP joints and extension of the MCP joints to retrieve the cereal from the horizontal slot.

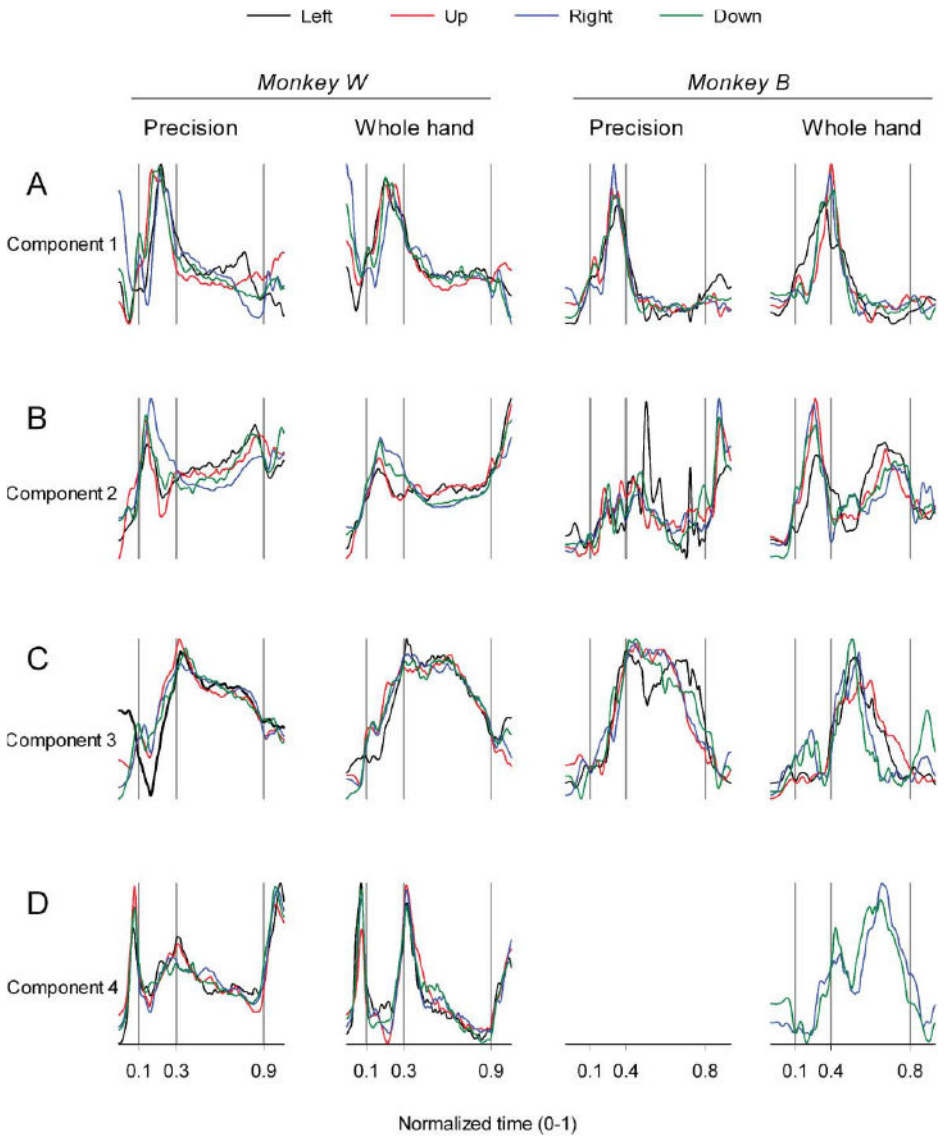

Figure 2.

Temporal scaling coefficients of muscle components. A-D: Plots of scaling coefficients as a function of time for the first four muscle components extracted from the data recorded during each of the 8 task conditions in both monkeys. Ordinate scales are arbitrary but uniform throughout. Time is normalized on a scale from 0-1. Behavioral event times are indicated by the vertical lines: reach onset, reach offset / grasp onset, grasp offset, respectively. A and B: Transport/preshape-related components (component 1 and component 2) were identified for all task conditions in both monkeys. C and D: Grasp-related components. Component 3 was identified for all task conditions in both monkeys. Component 4 was identified for all task conditions in monkey W and for the right and down targets in the whole-hand task in monkey B.

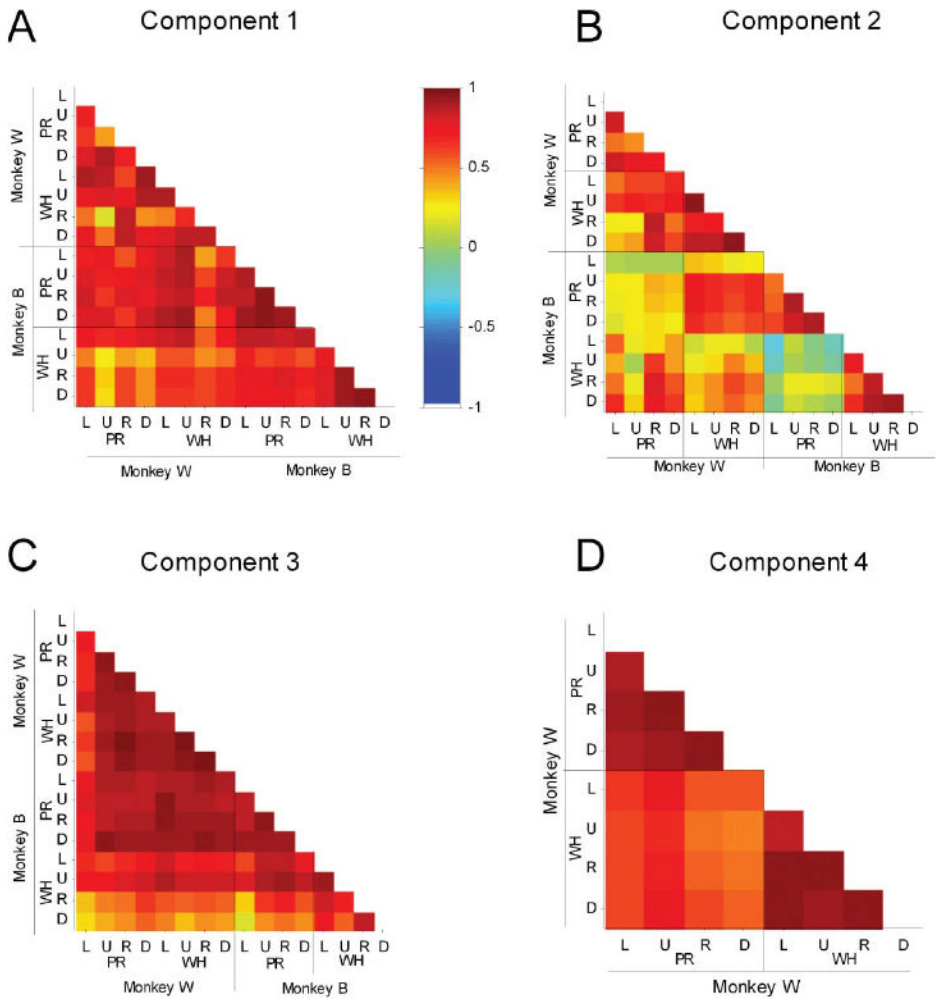

Figure 3.

Invariance of temporal scaling coefficients of muscle components. A-D: Color matrices summarize pairwise correlation coefficients between temporal scaling coefficients for the first four components extracted from data recorded during each of the 8 task conditions in monkeys. L, U, R, and D: left, up, right, down target locations, respectively; PR, WH: precision and whole-hand tasks, respectively. Note scale of color bar: -1 to C1. Scaling coefficients for component 1 (A) and component 3 (C) were conserved well across tasks and across monkeys. Scaling coefficients for component 2 (B) were relatively conserved within an animal for a given grasp type; results were mixed for comparisons across animals. Activation waveforms for component 4 (D, in monkey W only) were more strongly correlated for a given grasp type than across grasp types.

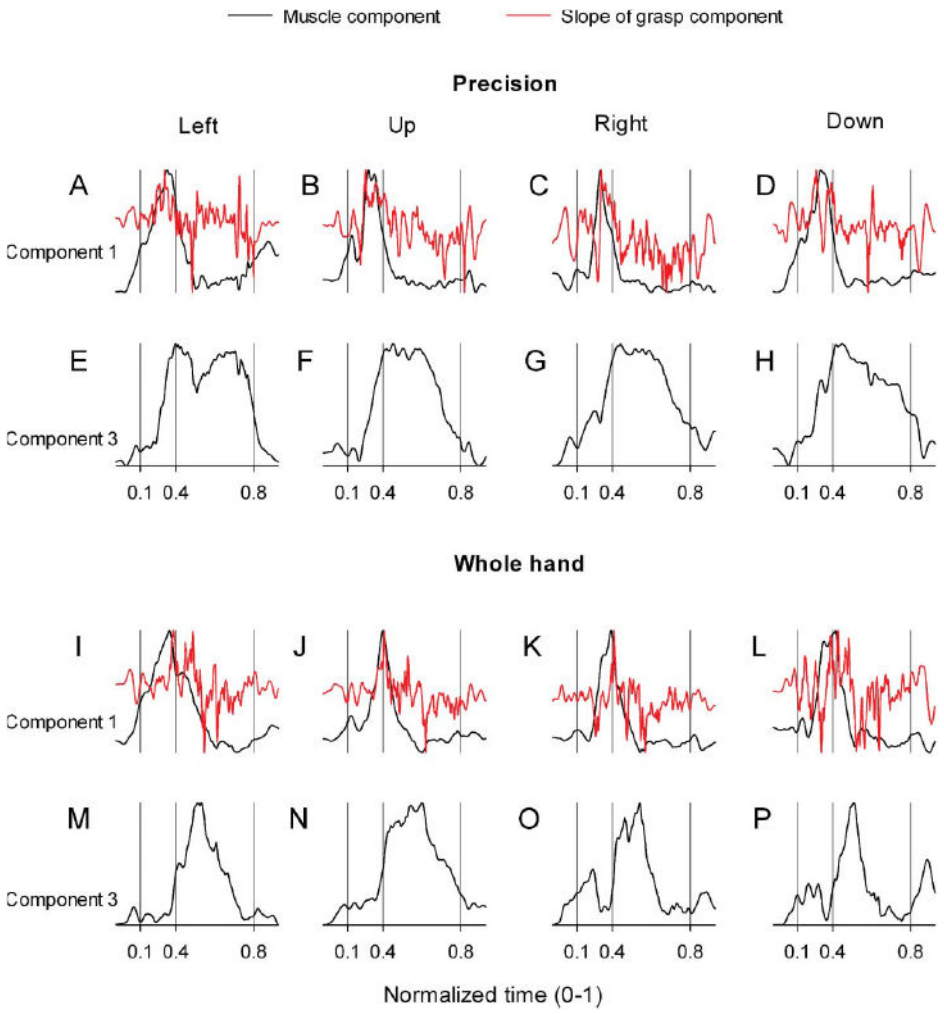

Figure 4.

Temporal coupling between scaling coefficients of transport/preshape- and grasp-related components. A-P: Plots of scaling coefficients as a function of time for transport/preshape-related component 1 (A-D and I-L) and grasp-related component 3 (E-H and M-P) for precision (A-H) and whole-hand (I-P) tasks to left, up, right, and down target locations in monkey W. Records of slope of the scaling coefficients for component 3 are overplotted (red) on the scaling coefficients for component 1 (Fig. 8, A–D and I–L). Ordinate scales are arbitrary but uniform throughout. Time scale is normalized. Behavioral event times are indicated by the vertical lines: reach onset, reach offset / grasp onset, grasp offset, respectively.

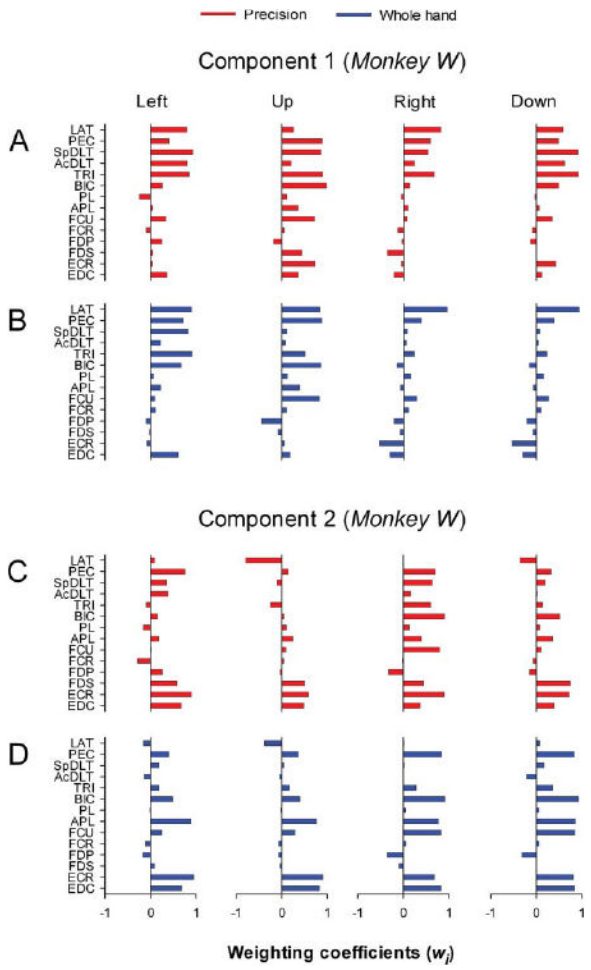

Figure 5.

Weighting coefficients of transport/preshape-related muscle components in monkey W. A-D: Horizontal bar plots of the amplitude of weighting coefficients of component 1 (A-B) and component 2 (C-D) for precision and whole-hand tasks to left, up, right, and down target locations in monkey W. Weighting coefficients represent the muscle activation balance of synchronously activated muscles in particular ratios with respect to each other. For muscle abbreviations, see Table 1. Muscles are referred to by functional groups in text for clarity. Functional groupings are as follows: monkey W—proximal (LAT, PEC, SpDLT, AcDLT, TRI, BIC), wrist flexors (FCU, FCR), finger flexors (FDP, FDS), wrist-digit extensors (EDC, ECR); monkey B – proximal (TM, PEC, SpDLT, ClDLT, AcDLT, TRI, BR, BIC), wrist flexors (FCU, FCR), finger flexors (FDP, FDS), and wrist-digit extensors (ECU, ED45, ED23, EPL, ECR, EDC).

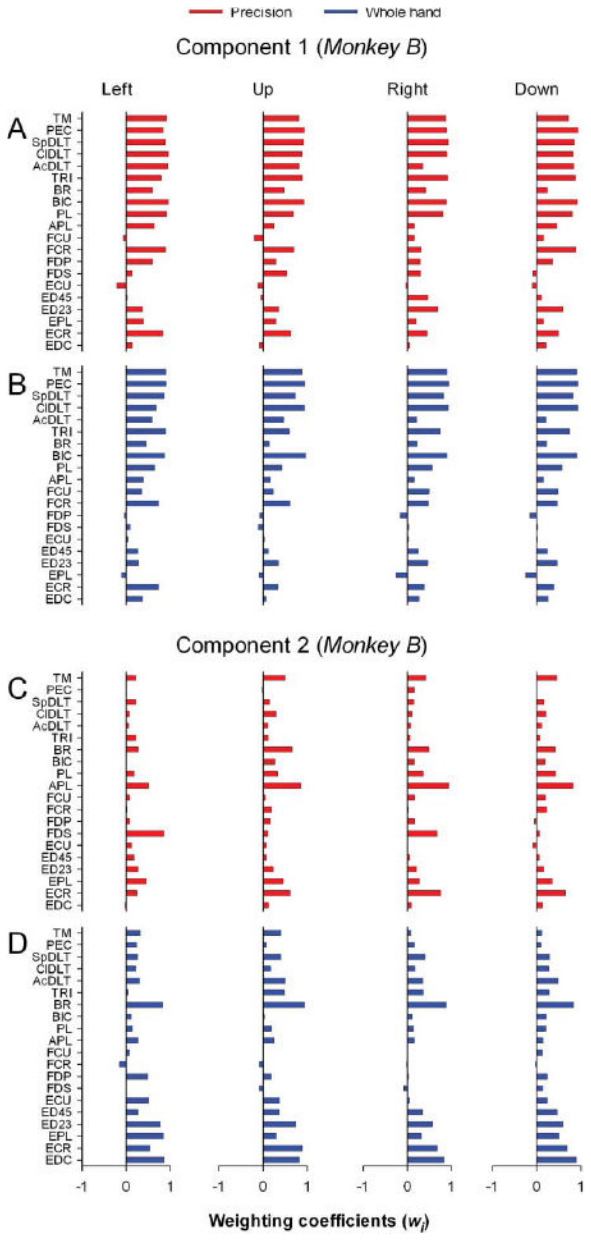

Figure 6.

Weighting coefficients of transport/preshape-related muscle components in monkey B. A-D: Horizontal bar plots of the amplitude of weighting coefficients of component 1 (A-B) and component 2 (C-D) for precision and whole-hand tasks to left, up, right, and down target locations.

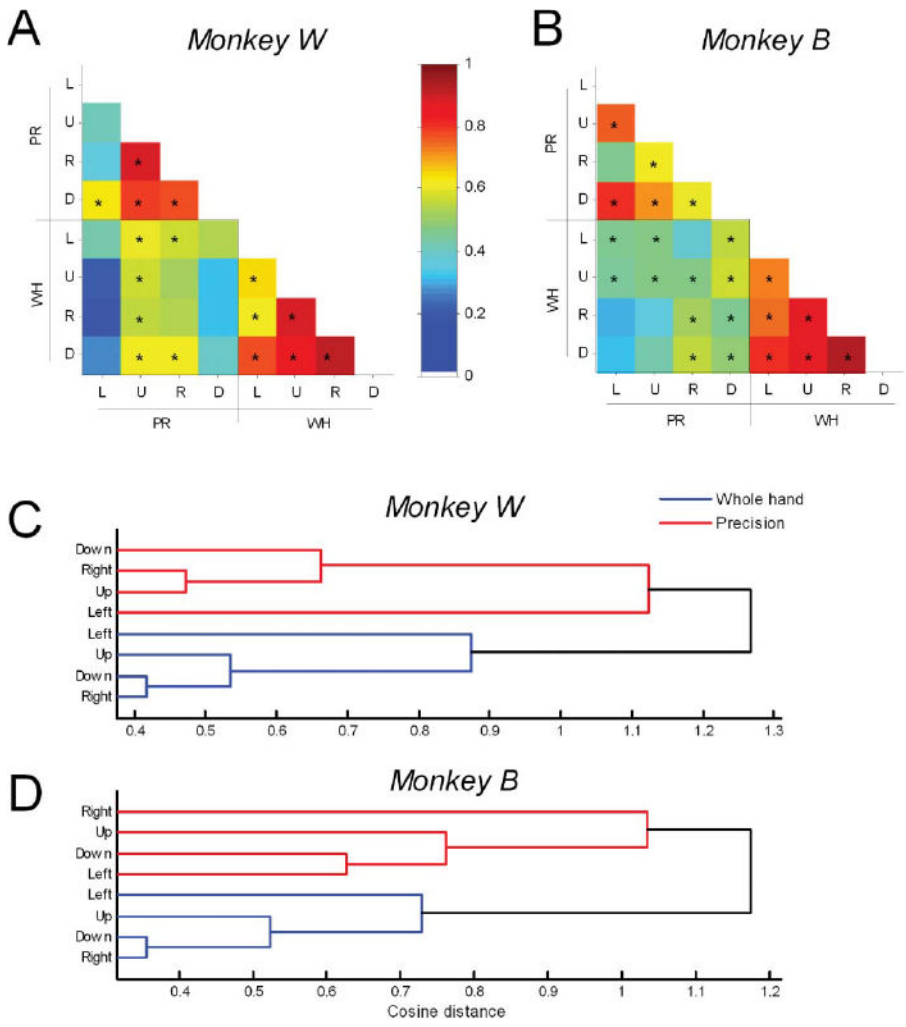

Figure 7.

Strength of association (similarity) of transport/preshape-related muscle components. A-B: Color matrices summarize Rv-coefficients for pairwise correlations of weighting coefficients in both precision and whole-hand tasks in monkey W (A) and monkey B (B). Rv-coefficients were higher and, therefore, strength of association (similarity) was higher when reaches shared the same grasp type than when they shared the same target location. Note scale of color bar: 0 to +1. L, U, R, and D: left, up, right, down target locations, respectively; PR, WH: precision and whole-hand tasks, respectively. Asterisk (*) in a given square of color matrix denotes statistically significant -coefficient for the particular pair-wise comparison ($p < 0.001$, adjusted for multiple comparisons). C-D: Dendrograms resulting from hierarchical cluster analysis of transport/preshape-related components of monkey W (C) and monkey B (D). Vertical lines indicate nodes at which the clustering algorithm merges clusters. Horizontal distances between vertical lines reflect the cosine distances between merged clusters. The smaller the horizontal distance at which clusters merge, the closer together (in cosine space) the clusters are, and thus more similar the objects in the clusters are. The sequence of merging of clusters in the whole-hand task was the same for both animals - components from right and down target locations were most similar and

merged into a single cluster, followed by components to the up and left target locations. Transport/preshape-related components were more similar for a given grasp type than for a given target location.

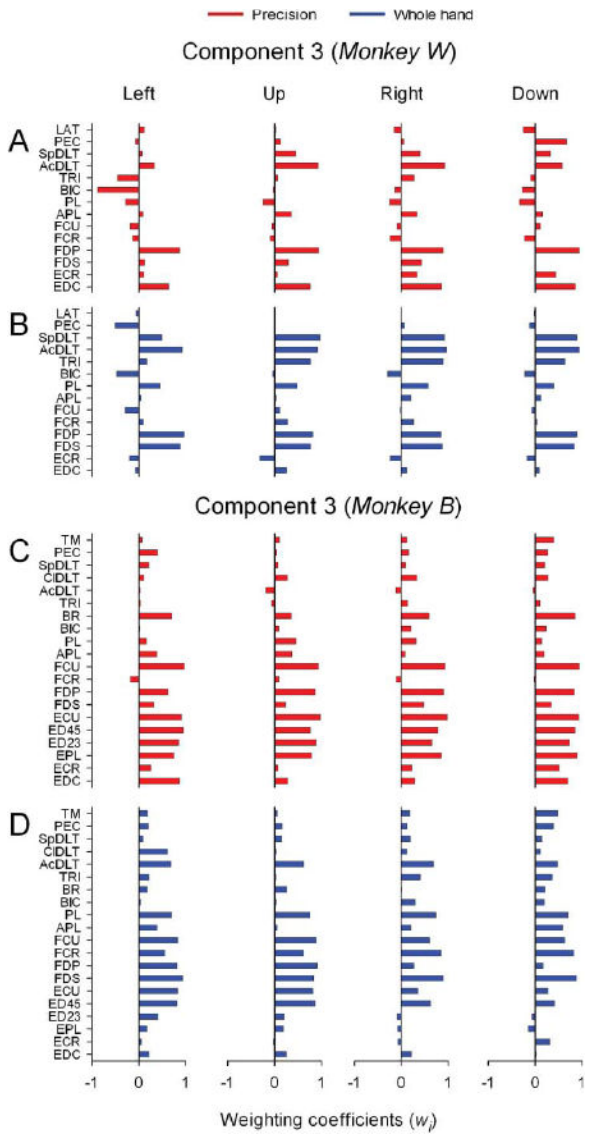

Figure 8.

Spatial structure of grasp-related muscle component 3. A-D: Horizontal bar plots of the amplitude of weighting coefficients of component 3 for precision and whole-hand tasks to left, up, right, and down target locations in monkey W (A-B) and monkey B (C-D).

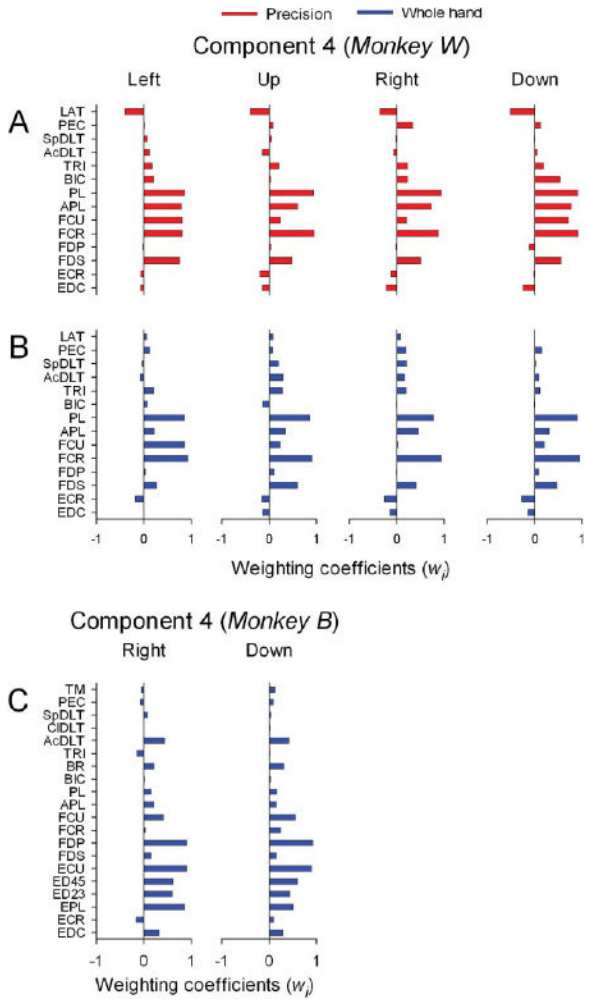

Figure 9.

Spatial structure of grasp-related muscle component 4. A-D: Horizontal bar plots of the amplitude of weighting coefficients of component 3 for precision and whole-hand tasks to left, up, right, and down target locations in monkey W (A-B) and for whole-hand task to right and down target locations in monkey B (C).

Table 1

Recording of EMG activity from forelimb muscles.

Muscle		EMG recording frequency	
Digits	**Abbreviation**	**Monkey B**	**Monkey W**
Extensor digitorum communis	EDC	3/5	7/7
Extensor digitorum two and three	ED23	3/5	
Extensor digitorum four and five	ED45	1/5	2/7 *
Flexor digitorum superficialis	FDS	1/5	6/7
Flexor digitorum profundus	FDP	2/5	3/7
Extensor pollicis longus	EPL	1/5	
Palmaris longus	PL	3/5	3/7
Wrist			
Extensor caripii radialis	ECR	3/5	6/7
Extensor carpii ulnaris	ECU	3/5	
Flexor carpii radialis	FCR	3/5	6/7
Flexor carpii ulnaris	FCU	4/5	2/7
Elbow			
Brachioradialis	BR	2/5	
Biceps	BIC	2/5	2/7
Triceps	TRI	2/5	4/7
Shoulder			
Acromion deltoid	AcDLT	2/5	5/7
Spino deltoid	SpDLT	2/5	4/7
Cleido deltoid	ClDLT	2/5	
Pectoralis	PEC	2/5	4/7
Teres major	TM	2/5	
Latissimus dorsii	LAT		2/7

EMG activity of 14 and 20 forelimb muscles was recorded in monkey W and monkey B, respectively. 7 recording sessions over a 9-day period were conducted in monkey W, and 5 recording sessions over a 7-day period were conducted in monkey B. In each of the 12 recording sessions, EMG activity of 9 muscles was recorded simultaneously. Numerical entries for a given muscle indicate EMG recording frequency, i.e. number of recording sessions for the given muscle over the total number of recording sessions in the animal.

* Muscle ED45 was recorded in 2/7 recording sessions in monkey W, however those data were not used in the analyses because of technical difficulties.

Table 2

Percent variance accounted for by muscle components.

Task Conditions		Monkey W	Monkey B	
Precision	Left	85.5% (4)	89.9% (4)	
	Up	86.7% (4)	84.9% (4)	91.7% (5)
	Right	87.5% (4)	86.3% (4)	93.2% (5)
	Down	85.4% (4)	87.5% (4)	90.7% (5)
Whole hand	Center	90.4% (4)	89.5% (4)	92.7% (5)
	Up	90.1% (4)	84.4% (4)	93.1% (6)
	Right	90.0% (4)	83.8% (4)	91.4% (5)
	Down	90.3% (4)	86.5% (4)	92.8% (5)

Note. The *n* values are listed in parentheses.

Percent variance accounted for (%VAF). Number in parentheses (n) refers to the number of components in the factor extraction. The %VAF by 4 components in Monkey B is shown for comparison with Monkey W.

Table 3

Temporal coupling between transport/preshape- and grasp-related muscle components.

		Normalized time (0–1 timescale)	
		Time of peak activation of component 1 (transport/ preshape-related)	Time of peak slope of component 3 (grasp-related)
Precision			
Monkey W	Left	0.25	0.25
	Up	0.20	0.20
	Right	0.25	0.23
	Down	0.24	0.27
Monkey B	Left	0.31	0.30
	Up	0.28	0.26
	Right	0.29	0.30
	Down	0.29	0.27
Whole hand			
Monkey W	Left	0.24	0.22
	Up	0.24	0.22
	Right	0.20	0.24
	Down	0.24	0.25
Monkey B	Left	0.33	0.35
	Up	0.37	0.37
	Right	0.36	0.38
	Down	0.39	0.36